FEBS Letters 346 (1994) 251–256

FEBS 14097

Molecular cloning and functional expression of a novel brain-specific inward rectifier potassium channel

Ken-Ichirou Morishige[a], Naohiko Takahashi[a,c], Arshad Jahangir[a], Mitsuhiko Yamada[a,c], Hidekazu Koyama[a], Jill S. Zanelli[a], Yoshihisa Kurachi[a,b,c,*]

[a]*Division of Cardiovascular Diseases, Department of Internal Medicine, Mayo Clinic, Rochester, MN 55905, USA*
[b]*Department of Pharmacology, Mayo Clinic, Rochester MN 55905, USA*
[c]*Department of Pharmacology II, Osaka University Medical School, Suita, Osaka 565, Japan*

Received 18 March 1994; revised version received 29 April 1994

Abstract

We have cloned a novel brain-specific inward rectifier K^+ channel from a mouse brain cDNA library and designated it MB-IRK3. The mouse brain cDNA library was screened using a fragment of the mouse macrophage inward rectifier K^+ channel (IRK1) cDNA as a probe. The amino acid sequence of MB-IRK3 shares 61% and 64% identity to MB-IRK1 and RB-IRK2, respectively. *Xenopus* oocytes injected with cRNA derived from this clone expressed a potassium current which showed inward-rectifying channel characteristics similar to MB-IRK1 and RB-IRK2 currents, but distinct from ROMK1 or GIRK1 current. However, the single channel conductance of MB-IRK3 was ~10 pS with 140 mM extracellular K^+, which was distinct from that of MB-IRK1 (20 pS). MB-IRK3 mRNA expressed specifically in the forebrain, which clearly differed from MB-IRK1 and RB-IRK2 mRNAs. These results indicate that members of the IRK family with distinct electrophysiological properties express differentially and may play heterogenous functional roles in brain functions.

Key words: Inward rectifier potassium channel; cDNA library; Mouse brain; Northern blot analysis; *Xenopus* oocyte

1. Introduction

Complementary DNAs of background or inward-rectifying potassium channels have been cloned from the outer medulla of rat kidney (ROMK1) [1] and from a mouse macrophage cell line (IRK1) [2]. Both of these channels show two transmembrane segments with one pore-forming region. The G protein-coupled muscarinic potassium channel (GIRK1), recently cloned from rat heart, also possesses essentially the same molecular structure [3]. Northern blot analysis shows ROMK1 mRNA to be expressed in kidney, spleen, lung, eye and forebrain [1], IRK1 in forebrain, cerebellum, heart, skeletal muscle and a macrophage cell line [2], and GIRK1 in forebrain, cerebellum and heart [3]. These K^+ channels can also be electrophysiologically distinguished from each other at the whole cell and single channel current levels.

We recently cloned the second member of IRK family from rat brain cDNA library and designated it RB-IRK2 [4]. Although RB-IRK2 currents expressed in *Xenopus* oocytes show electrophysiological properties similar to IRK1 current, RB-IRK2 mRNA expresses highly in cerebellum, and moderately in forebrain, heart and skeletal muscle, which is distinct from the distribution of IRK1 [4]. Thus, the members of the IRK family may play multiple functional roles in various organs.

In the present study, to elucidate further diversity of the IRK family in the central nervous system and possible functional differences among the members, we have cloned from the mouse brain cDNA library, electrophysiologically characterized and examined organ distribution of a novel member of the IRK family and compared its electrophysiological properties and distribution with those of MB-IRK1 and RB-IRK2.

2. Materials and methods

2.1. Screening of mouse brain cDNA library and DNA sequencing

A mouse brain cDNA library was screened under a mild stringency conditions using a *Bst*XI–*Not*I digested IRK1 (~3.8 kb) as a probe. Mouse IRK1 cDNA was kindly provided by Dr. Lily Y. Jan (UCSF, San Francisco, CA) [2]. 4×10^6 Phage clones were screened with a ^{32}P-labelled probe. Hybridization was conducted in 5 × SSC, 30% formamide, 0.08% bovine serum albumin, 0.08% Ficoll, 0.08% polyvinylpyrrolidone, 0.1% sodium dodecyl sulfate (SDS) and 200 μg/ml denatured salmon sperm DNA, at 37°C for 17 h. Filters were washed once with 1 × SSC, 0.1% SDS at room temperature for 15 min and then twice with 0.1 × SSC, 0.5% SDS at room temperature for 20 min, and finally exposed to an X-ray film overnight at −70°C with an intensifying screen. DNA sequencing was performed on both strands using a sequencing kit (USB, Cleveland, OH) by specific oligonucleotide primers as previously described [5].

*Corresponding author. Department of Pharmacology II, Osaka University Medical School, Suita, Osaka 565, Japan. Fax: (81) (6) 879 3519.

Abbreviations: IRK, inward rectifier potassium channel; cDNA, complementary deoxyribonucleic acid; cRNA, complementary ribonucleic acid; mRNA, messenger ribonucleic acid; SSC, saline-sodium citrate; SDS, sodium dodecyl sulfate; GAPDH, glyceraldehyde-3-phosphate-dehydrogenase.

SSDI 0014-5793(94)00483-C

2.2. *Functional expression of a mouse brain inward rectifier potassium channel in* Xenopus *oocytes*

The positive clone obtained was transcribed in vitro by T_3 RNA polymerase after digestion with *XhoI* [5]. This transcript was dissolved in sterile water, and injected 50 nl of 1 μg/μl to manually defoliculated oocytes. After injection, oocytes were incubated in a modified Barth solution at 18°C, and electrophysiological studies were undertaken 48–96 h later.

Two-electrode voltage clamp experiments were carried out with a commercially available amplifier (Turbo Clamp TEC 01C, Tamm, Germany) with microelectrodes which, when filled with 3 M KCl, had resistances of 0.5–1.5 MΩ. Oocytes were bathed in a solution which contained 90 mM KCl, 3 mM $MgCl_2$, 5 mM HEPES (pH 7.4) and 150 μM niflumic acid to block endogenous chloride current. Oocytes were voltage-clamped at various holding potentials and voltage-steps of 1.5 s duration were applied to the cells in 10 mV increments every 5 s. Experiments were performed at room temperature (20–22°C). Single channel recordings were made in the cell-attached patch configuration using a patch clamp amplifier (Axopatch 200A, Axon Instruments, Foster City, CA). Both pipette and bath solutions contained 140 mM KCl, 1.4 mM $MgCl_2$ and 10 mM HEPES (pH adjusted to 7.4 with KOH). Experiments were performed at room temperature (20–22°C). Electrophysiological data were stored on video tapes using a PCM data recording system (NF Electronic Design, Tokyo, Japan), and subsequently replayed for computer analysis (EP Analisis, Human Intelligence Inc., Rochester, MN).

2.3. *Northern blot analysis*

Total RNAs from various organs were extracted by the guanidine thiocyanate method [7], and poly(A)$^+$ RNAs were isolated using Oligotex-dT mRNA kit (QIAGEN, Chatsworth, CA). Equal amounts (3 μg) of poly(A)$^+$ RNAs, as determined by absorbance at 260 nm, were separated in 1% agarose-formaldehyde gel and transferred to a Hybond-N nylon membrane (Amersham, Arlington Heights, IL). Hybridization using the random primer labeled probe was performed in 50% formamide hybridization buffer with *NotI* digested fragment (1.4

A

```
                                                                                 5'- GCA
CGA CCG GAC ACT CGC CGC CCA GAC CCT CCT CGG ACC TTA CGC CCC GGG GCC CTG CAT CTC CCC AGG TGA CCA CGA CGA CGT CCT CAG GTC    -1

ATG CAC GGA CAC AAC CGA AAC GGG CAG GCC CAC GTG CCC AGG CGG AAA CGC CGC AAC CGC TTT GTC AAG AAG AAC GGC CAG TGT AAC GTC    90
Met His Gly His Asn Arg Asn Gly Gln Ala His Val Pro Arg Arg Lys Arg Arg Asn Arg Phe Val Lys Lys Asn Gly Gln Cys Asn Val    30

TAC TTC GCC AAC CTG AGC AAC AAG TCC CAG CGC TAC ATG GCA GAC ATC TTC ACC ACC TGC GTG GAC ACG CGC TGG CGC TAT ATG CTC ATG   180
Tyr Phe Ala Asn Leu Ser Asn Lys Ser Gln Arg Tyr Met Ala Asp Ile Phe Thr Thr Cys Val Asp Thr Arg Trp Arg Tyr Met Leu Met    60

ATC TTC TCC GCG GCC TTC CTC GTT TCC TGG CTC TTC TTC GGC CTC CTC TTC TGG TGG ATT GCC TTC TTC CAT GGT GAC CTG GAG GCC AGT   270
Ile Phe Ser Ala Ala Phe Leu Val Ser Trp Leu Phe Phe Gly Leu Leu Phe Trp Trp Ile Ala Phe Phe His Gly Asp Leu Glu Ala Ser    90
                           M1
CCC TCT GTG CCC GCG GTA GGA GGC CCG GGG GGC AAT GGC GGG GAA AGC CCG AAT GCC CCC AAA CCC TGT ATC ATG CAC GTA AAC GGC TTT   360
Pro Ser Val Pro Ala Val Gly Gly Pro Gly Gly Asn Gly Gly Glu Ser Pro Asn Ala Pro Lys Pro Cys Ile Met His Val Asn Gly Phe   120

TTG GGG GCC TTC CTC TTC TCA GTG GAG ACC CAG ACG ACC ATT GGC TAC GGG TTC CGG TGT GTG ACA GAG GAG TGC CCG TTG GCG GTC ATT   450
Leu Gly Ala Phe Leu Phe Ser Val Glu Thr Gln Thr Thr Ile Gly Tyr Gly Phe Arg Cys Val Thr Glu Glu Cys Pro Leu Ala Val Ile   150
                           H5
GCG GTG GTT GTC CAG TCC ATT GTG GGC TGT GTC ATT GAC TCC TTC ATG ATT GGC ACG ATC ATG GCC AAG ATG GCA CGG CCC AAG AAG CGG   540
Ala Val Val Val Gln Ser Ile Val Gly Cys Val Ile Asp Ser Phe Met Ile Gly Thr Ile Met Ala Lys Met Ala Arg Pro Lys Lys Arg   180
                      M2
GCA CAG ACC CTG CTG TTC AGC CAC CAT GCT GTC ATC TCC GTT CGA GAC GGC AAG CTC TGC CTG ATG TGG CGC GTG GGT AAC CTG CGC AAG   630
Ala Gln Thr Leu Leu Phe Ser His His Ala Val Ile Ser Val Arg Asp Gly Lys Leu Cys Leu Met Trp Arg Val Gly Asn Leu Arg Lys   210

AGT CAC ATT GTG GAG GCC CAC GTC CGG GCC CAG CTC ATC AAA CCC TAC ATG ACA CAG GAG GGT GAG TAC CTG CCA CTG GAC CAG CGG GAC   720
Ser His Ile Val Glu Ala His Val Arg Ala Gln Leu Ile Lys Pro Tyr Met Thr Gln Glu Gly Glu Tyr Leu Pro Leu Asp Gln Arg Asp   240

CTC AAC GTG GGC TAT GAC ATC GGC CTG GAC CGC ATC TTC TTG GTG TCA CCC ATC ATC ATA GTG CAT GAA ATC GAC GAG GAC AGC CCA CTC   810
Leu Asn Val Gly Tyr Asp Ile Gly Leu Asp Arg Ile Phe Leu Val Ser Pro Ile Ile Ile Val His Glu Ile Asp Glu Asp Ser Pro Leu   270

TAC GGC ATG GGC AAG GAG GAG CTG GAG TCA GAG GAC TTT GAG ATT GTG GTC ATC CTG GAG GGT ATG GTG GAG GCC ACG GCT ATG ACC ACT   900
Tyr Gly Met Gly Lys Glu Glu Leu Glu Ser Glu Asp Phe Glu Ile Val Val Ile Leu Glu Gly Met Val Glu Ala Thr Ala Met Thr Thr   300

CAG GCC CGC AGC TCC TAT CTG GCC AGT GAG ATC CTG TGG GGT CAC CGG TTT GAG CCT GTG GTC TTC GAG GAA AAG AGT CAC TAC AAG GTG   990
Gln Ala Arg Ser Ser Tyr Leu Ala Ser Glu Ile Leu Trp Gly His Arg Phe Glu Pro Val Val Phe Glu Glu Lys Ser His Tyr Lys Val   330

GAC TAC TCA CGA TTC CAC AAG ACC TAT GAG GTG GCT GGC ACG CCT TGC TGC TCC GCC CGT GAG CTG CAG GAG AGC AAG ATC ACG GTG CTG  1080
Asp Tyr Ser Arg Phe His Lys Thr Tyr Glu Val Ala Gly Thr Pro Cys Cys Ser Ala Arg Glu Leu Gln Glu Ser Lys Ile Thr Val Leu   360

CCC GCC CCA CCG CCC CCT CCC AGT GCC TTC TGC TAT GAG AAT GAG CTG GCC CTT ATG AGC CAG GAG GAA GAG GAG ATG GAA GAG GAG GCT  1170
Pro Ala Pro Pro Pro Pro Pro Ser Ala Phe Cys Tyr Glu Asn Glu Leu Ala Leu Met Ser Gln Glu Glu Glu Glu Met Glu Glu Glu Ala   390

GCG GCC GCA GCA GCC GTG GCT GCA GGC CTG GGC CTG GAG GCA GGT TCC AAA GAG GAG GCA GGC ATT ATC CGG ATG CTT GAG TTT GGC AGC  1260
Ala Ala Ala Ala Ala Val Ala Ala Gly Leu Gly Leu Glu Ala Gly Ser Lys Glu Glu Ala Gly Ile Ile Arg Met Leu Glu Phe Gly Ser   420

CAC CTG GAT CTG GAG CGC ATG CAA GCC GCC ACC CTT CCA CTG GAC AAT ATT TCC TAT CGC AGG GAA TCT CGC ATC TGA CCT CCA GGC CCT  1350
His Leu Asp Leu Glu Arg Met Gln Ala Ala Thr Leu Pro Leu Asp Asn Ile Ser Tyr Arg Arg Glu Ser Arg Ile                      445

GCC CTC CTC TAT TCC CGC AAG AGC CTC TGC CAG GGG TGG GAC GAC AGG ACA AGC CTT CCA CTC TTA GGA CAG AGT TGA ACG TGG CTC TGT  1440
GGA CCT AGA GGA AGG TGG GGG CTT CCA AGA CTG GGA GAT CCC TTC CTG TTG ACT ACA GGG CCC AGG ACT GGA AAG GAC CCA GGT ACT CCG  1530
CCC TGA TGG CCC AGG CCC CCC TGG CAT CTC CCC ACG GTG GCT CTG GGC CCC CAG ATC TTC CAC CCT TTT CCC ACT GAC CCT TCA AGG ATG  1620
TAC CCC TTC TGC TCT CAG GAC CTC GGG GAA GCC GGC TGG ACT CCT GGG GGG CGG GCA TCA TGG GGT TCT GGG TGG CCA GGG TGG GTC TGG  1710
GGG AGG GGG AAG GGT GTG TTT CTT TTG CAT GAC TGT GGT CTG TGC TCT TGA TTC TCT TTT TGT AAA TAT CTA TAA ATG GGA GAG ATG GAG  1800
ACA CAA GTC CAC CTC TGC CCA TTT CTA CCT GTG AGA ACA GAG AGA GGC TGC CAA CCC CTC TCT GTG CAC TCC CCC GTC CAG CCT CAG CCC  1890
GAC CCA GCT GGC TGG TCC CTT GAG ACC TTT GAA GCC GGC TCT GTA TGG TGT TGG GTT TGG GTA CAG ACG GGA CTC AGA GGT AGG ATG AGT  1980
ACC CCT CCC TCC TTG CAG TCC CTC CAG TTT CCA GAT TGA TGA CGG CGT TTG TAA CTA TTT TTA ATA AAG CAT ATG GTC CAC TAA AAA AAA  2070
                                                                                                                         2074
AAA A
```

Fig. 1. (A) The nucleotide sequence and deduced amino acid sequence of the MB-IRK3 cDNA. The amino acids are numbered starting at the Met of the predicted amino terminus. The nucleotides are numbered at the side of the sequence. Positive numbers are assigned to nucleotides 3′ to the A of the initiation codon, which is assigned as +1. Nucleotides 5′ to this codon are assigned negative numbers. There is one potential cAMP and cGMP-dependent protein kinase phosphorylation site (443S), five potential protein kinase C phosphorylation sites (36S, 39S, 193S, 348S and 438S) and no potential tyrosine kinase phosphorylation sites. Possible membrane spanning regions (M1 and M2) and potential pore-forming region (H5) are indicated by lines below the sequence. (B) Alignment of the amino acid sequences (single letter code) of MB-IRK3 and MB-IRK1. Colons indicate amino acids identical with those in MB-IRK3. Dashes indicate gaps introduced into the sequence to improve alignment. The proposed transmembrane regions (M1 and M2) and potential pore-forming region H5 are boxed.

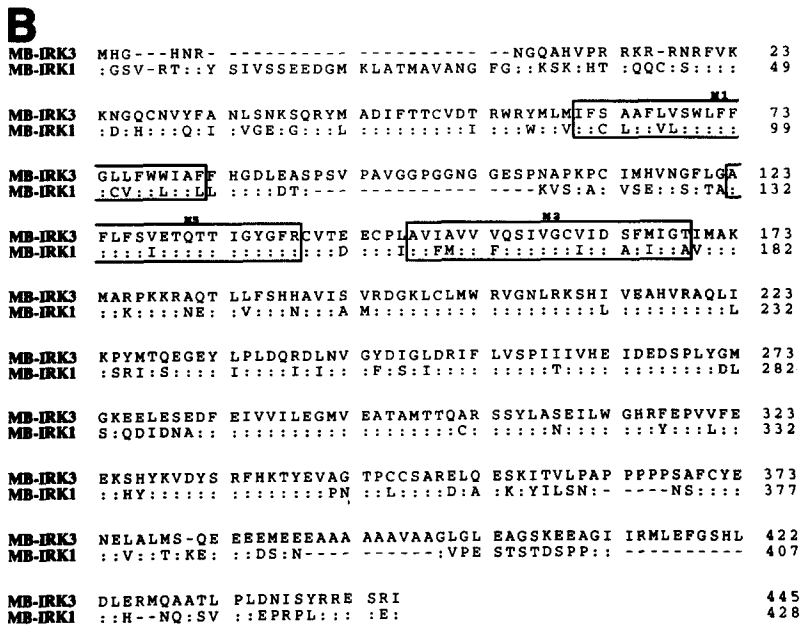

Fig. 1 (*continued*).

kb) of pMB-IRK3 at 42°C. Glyceraldehyde-3-phosphate-dehydrogenase (GAPDH) cDNA probe was used as control to ascertain that equivalent amounts of mRNA had been transferred. Blots were washed at moderate stringency (55°C, 0.5 × SSC, 0.1% SDS) for 15 min and exposed to Kodak XAR-5 film with an intensifying screen at −70°C.

3. Results

3.1. Molecular cloning of a novel inward rectifier potassium channel

To identify a novel inward rectifying K^+ channel expressed in mammalian brain, we screened mouse brain cDNA library using the part of IRK1 cDNA which corresponded to amino acid sequences that contained the coding region of IRK1. We obtained IRK1 cDNA clones and the MB24 clone (1.1 kb) which contained a sequence similar to but distinct from that of the membrane spanning region of IRK1. Using the *Apa*I–*Sac*I digested fragment (0.8 kb) of pMB24, we screened 5×10^6 mouse brain cDNA clones. After this second screening, we obtained 25 cDNA clones. Analysis using restriction mapping suggested that the majority of these cDNAs are identical. We chose the cDNA clone with the longest 5′ untranslated region, and sequenced and expressed it in *Xenopus* oocytes. The size of this cDNA (MB24–29) was 2.5 kb which contained an open reading frame (1,335 bp) (Fig. 1). The deduced protein was cosisted of 445 amino acids, and the predicted molecular weight of the primary translation product was 59 kDa. We designated this clone MB-IRK3, based on its sequence (Fig. 1) and the electrophysiological properties of the expressed current (Fig. 2). The deduced amino acid sequence of MB-IRK3 revealed a number of potentially biologically significant sites for posttranslational modification (Fig. 1).

The deduced amino acid sequence of MB-IRK3 showed 61% and 64% identity with those of MB-IRK1 and RB-IRK2, respectively, but only 38% and 43% identity with those of rat ROMK1 and rat GIRK1, respectively. The Kyte–Doolittle hydropathy plot [8] of MB-IRK3 indicates two potential membrane spanning hydrophobic segments (M1 and M2) with a pore forming region (H5), a structure common to MB-IRK1 (Fig. 1B), RB-IRK2, ROMK1 and GIRK1 (data not shown) [1–4,6].

3.2. Whole cell current of Xenopus oocytes injected with MB-IRK3 cRNA

Fig. 2 illustrates the results obtained from a *Xenopus* oocyte which had been injected with cRNA derived from MB-IRK3 clone 72 h before the recording. In the bathing solution containing 90 mM K^+ ($[K^+]_o$) (top traces in Fig. 2A,C,E), hyperpolarizing voltage steps from a holding potential of 0 mV revealed rapid activation (< 10 ms) of large inward currents which showed little voltage-dependent inactivation even at extreme hyperpolarizing voltages. Upon depolarization the current showed a clear inwardly rectifying property.

The effect of $[K^+]_o$ on the MB-IRK3 current is depicted in Fig. 2A,B. As $[K^+]_o$ was lowered from 90 mM to 45, 20 and 10 mM, the slope conductance of MB-IRK3 current was decreased from 42.3 ± 2.5 μS to 35.1 ± 2.0, 30.6 ± 1.9, and 25.4 ± 2.4 μS (mean ± S.E., $n = 3$), respectively. The activation potential defined as the potential at which the slope conductance changes noticeably was in good agreement with the equilibrium

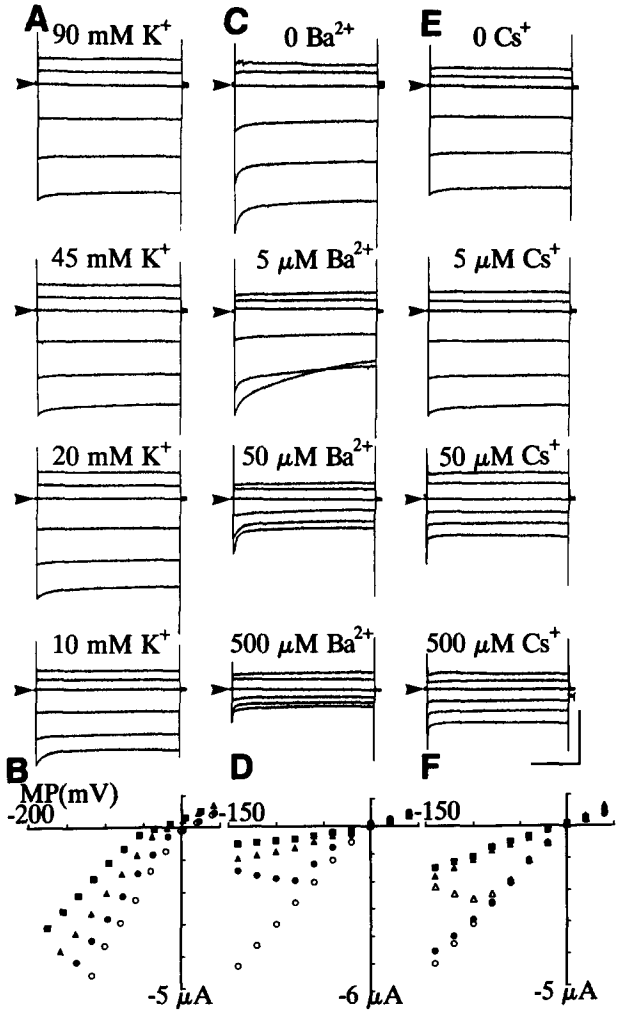

Fig. 2. Cell currents recorded from *Xenopus* oocytes expressing the MB-IRK3 clone. (A) The effect of varying external K^+ concentration. The holding potential was set at the zero current level in each solution, i.e. at 0 mV in 90 mM K^+, at −17.4 mV in 45 mM K^+, at −37.9 mV in 20 mM K^+, at −55.3 mV in 10 mM K^+ and at −78.4 mV in 4 mM K^+; the values correspond to the equilibrium potential for K^+ at each concentration of external K^+, with an assumption that the intracellular K^+ concentration of oocytes is 90 mM. Upper traces in each column show records obtained under control conditions. (A) The effect of external K^+ on the MB-IRK3 induced current. (B) Current–voltage relationship of the peak currents (10 ms after the start of voltage pulses) recorded from this oocyte at various K^+ concentrations. (C) The effect of external Ba^{2+}. (D) Current–voltage relationships of the steady-state currents recorded from this oocyte in the presence of Ba^{2+}. (E) The effects of external Cs^+. (F) Current–voltage relationships recorded in the presence of Cs^+. The time and cell current scales are applicable to all traces which were recorded from a single oocyte. Labels above each family of traces indicate the concentration of cations which had been included in the solution which bathed the oocytes. open circles: control; closed circle: 5 μM cation; open triangles: 30 μM, filled triangles: 50 μM cation; squares: 500 μM cation. Arrows indicate the zero current level.

potentials for K^+ (E_K) predicted from the Nernst equation at various $[K^+]_o$. Outward currents at potentials positive to E_K were considerably less than that predicted by a linear current–voltage relationship. These properties are consistent with those of the conventional type of inward rectifier potassium channels [9], including MB-IRK1 [2,6] and RB-IRK2 [4].

External Ba^{2+} (Figs. 2C,D) concentration-dependently induced a time- and voltage-dependent block of the inward currents expressed by MB-IRK3. At 5 and 50 μM, Ba^{2+} clearly induced the time- and voltage-dependent block with a comparatively small effect upon the instantaneous current (Fig. 2C), but a marked influence upon the steady-state current (Fig. 2D). At 500 μM, Ba^{2+} essentially abolished the inward currents, both instantaneous and steady state. All three concentrations of Ba^{2+} slightly reduced the outward currents recorded by voltage steps to positive membrane potentials.

Cs^+ (Fig. 2E,F) exhibited less of a time-dependent effect, when compared to Ba^{2+}, upon the MB-IRK3 current. It, however, showed a clear voltage-dependence of the block in a concentration-dependent manner (5–500 μM).

3.3. Single channel currents of MB-IRK3

Single channel currents flowing through MB-IRK3 were recorded in the cell-attached configuration from oocytes which had been injected with cRNA derived from MB-IRK3, 48–96 h before recording (Fig. 3). Currents passing through these channels were observed only in the inward direction and, thus, showed a strong inwardly rectifying property (Fig. 3A,B). As shown in Fig. 3B, the mean slope conductance of MB-IRK3 channel was 13.4 ± 2.1 pS (mean ± S.E.M., n = 5), significantly different from MB-IRK1 (~20 pS) and RB-IRK2 (~35 pS, unpublished data) [2, 6]. Thus, these three clones clearly expressed distinct inward-rectifying K^+ channels in *Xenopus* oocytes, although the difference was not clear at the whole cell current level.

3.4. Distribution of MB-IRK3 mRNA in various tissues

We conducted Northern blotting analysis of MB-IRK3 in various tissues. MB-IRK3 mRNAs (about 2.7 kb) was detected specifically in forebrain (cerebral hemispheres and diencephalon) and not in any other tissues, such as cerebellum, heart, skeletal muscle or kidney (Fig. 4). In addition, a very weak band of 5.5 kb was also detected in forebrain, which may result from alternative polyadenylation.

4. Discussion

In the present study, we described the amino acid sequence, electrophysiological characteristics and organ distribution of the third class of IRK family cloned from the mouse brain. The electrophysiological characteristics of this clone, i.e. such as absence of current at potentials positive to E_K, the dependence of the slope conductance on $[K^+]_o$, rapid activation upon hyperpolarizing pulses, and the time- and voltage-dependent block by Ba^{2+} and

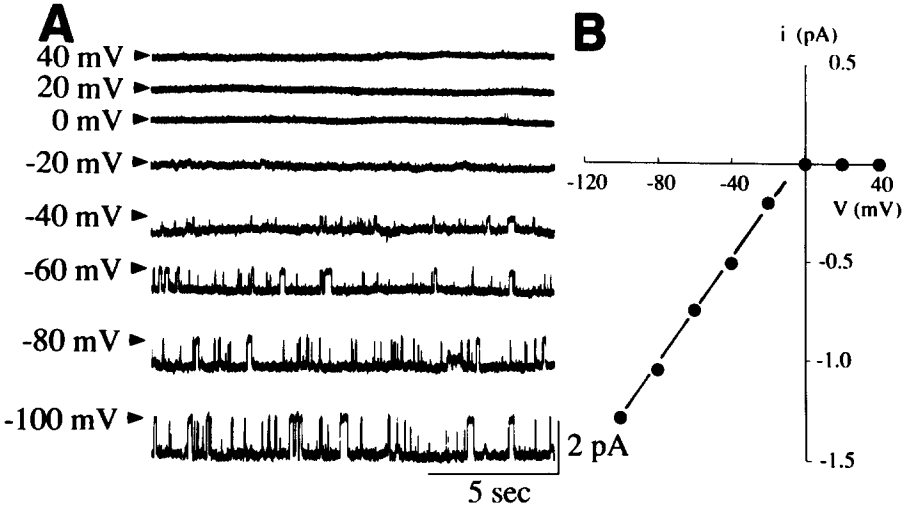

Fig. 3. Single channel recordings from cell-attached membrane patches of *Xenopus* oocytes expressing the MB-IRK3. (A) Membrane current traces recorded at the membrane potential values indicated to the left of each trace. The arrows to the right of certain traces indicate the patch current level recorded when all channels were closed. Each of these patches appeared to contain one inwardly rectifying potassium channel. The cut off frequency of the recording was 1 kHz (at −3 dB). (B) The current–voltage relationships of the channel records shown in (A).

Cs^+, were the same as those of classical inward rectifier potassium channels in a variety of cell types, including MB-IRK1 and RB-IRK2 [2,4,6]. The ROMK1 current expressed in oocytes does not rectify prominently [1]. Activation of G proteins is essential for the GIRKI current, which is also characterized with a slow activation time course upon hyperpolarizing pulses [3]. Thus, the obtained clone may belong to the same family as MB-IRK1 and RB-IRK2, but is distinct from ROMK1 or GIRK1. Consistently with this notion, the amino acid sequence of the clone shows 61% identity with mouse macrophage IRK1 [2], 64% with RB-IRK2 [4], 38% with rat kidney ROMK1 [1] and 43% with rat heart GIRK1 [3]. Therefore, we have designated it MB-IRK3.

Like all previously cloned inward rectifier potassium channels, the MB-IRK3 channel possesses two transmembrane domains with a putative pore-forming region (H5). The H5 region of MB-IRK3 comprises virtually identical amino acids with those present in MB-IRK1 (with the exception of residue 128) and RB-IRK2 (with the exception of residues 128 and 138). These differences in the amino acid sequences of the H5 region might be responsible for the difference in the unitary conductance among these channels, since MacKinnon and Yellen [10] showed that one amino acid substitution in the H5 region alters the single channel conductance of *Shaker*-related potassium channels. However, it was also indicated that the regions outside of H5 are involved in the regulation of single channel conductance of *Shaker*-related potassium channels [11,12]. Therefore, further studies such as site-directed mutagenesis of the amino acids are necessary for understanding the precise roles of the H5 region and other regions on the single channel conductance of IRK.

One of the most specific features of MB-IRK3 is its distribution among various organs which is distinct from those of MB-IRK1, RB-IRK2, GIRK1 and ROMK1;

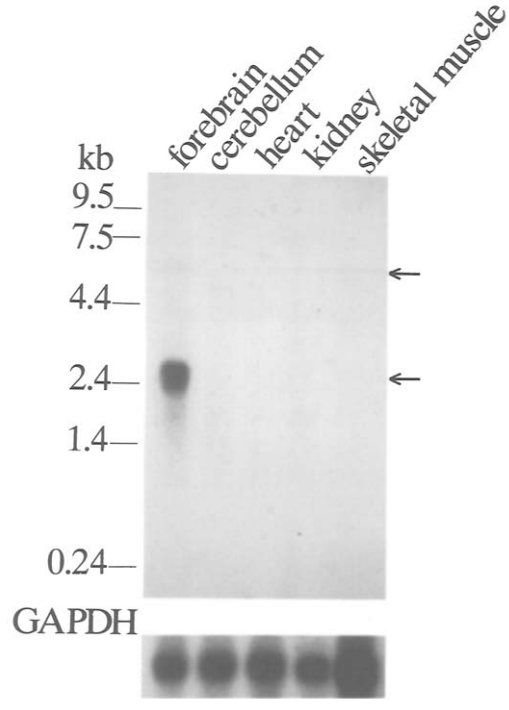

Fig. 4. Distribution of MB-IRK3 mRNA in various tissues by Northern blot analysis. The lane represent poly(A)$^+$ RNA from mouse forebrain, cerebellum, heart, kidney and skeletal muscle. *Not*I digested fragment (1.4 kb) of pMB-IRK3 was used for a probe. One major band of ~2.7 kb and the other weak band of ~5.5 kb mRNAs that hybridized with the probe are indicated with arrows. The positions of RNA size markers are shown on the left side. The quantity of RNA samples were standardized by reprobing the same blot with a labelled cDNA for GAPDH (lower panel).

i.e. MB-IRK3 mRNA is expressed only in the forebrain, whereas IRK1, RB-IRK2, GIRK1 and ROMK1 are expressed not only in the forebrain, but also in other peripheral tissues. This result further supports the notion that the MB-IRK3 is a novel member of IRK family.

This study provides an evidence that the IRK family is composed of at least three genes. There may exist other clones belonging to this family. The members of IRK family may distribute differentially in various cells and play multiple functional roles. Further studies are needed to elucidate these possibilities.

Acknowledgements: The authors thank Dr. Lily Y. Jan (UCSF, San Francisco, CA) for IRK1 clone and Dr. Nozomu Mori (USC, Los Angeles, CA) for his critical reading manuscript. This study was supported by NIH RO1 HL47360 to Y.K.. This work was performed during the tenure of the Established Investigatorship of the American Heart Association to Y.K.

References

[1] Ho, K., Nichols, C.G., Lederer, W.J., Lytton, J., Vassilev, P.M., Kanazirska, M.V. and Hebert, S.C. (1993) Nature 362, 31–38.
[2] Kubo, Y., Baldwin, T.J., Jan, Y.N. and Jan, L.Y. (1993) Nature 362, 127–133.
[3] Kubo, Y., Reuveny, E., Slesinger, P.A., Jan, Y.N. and Jan, L.Y.(1993) Nature 364, 802–806.
[4] Koyama, H., Morishige. K., Takahashi. N., Zanelli. J. S., Fass. D.N. and Kurachi. Y. (1994) FEBS Lett. (in press)
[5] Sugimoto, T., Tsuchimochi, H., McGregor, C.G.A., Mutoh, H., Simizu, T, and Kurachi, Y. (1992) Biochem. Biophys. Res. Commun. 189, 617–624.
[6] Morishige, K., Takahashi, N., Findlay, I., Koyama, H., Zanelli, J.S., Peterson, C., Jenkins, N.A., Copeland, N.G., Mori, N. and Kurachi, Y. (1993) FEBS Lett. 336, 375–380.
[7] Chirwin, J.M., Przybyla, A.E., MacDonald, R.J. and Rutter, W.J. (1979) Biochemistry 18, 5292–5299.
[8] Kyte, J. and Doolittle, R.F. (1982) J. Mol. Biol. 157, 105–132.
[9] Hagiwara, S., Miyazaki, S. and Rothenthal, N.P. (1976) J. Gen. Physiol. 67, 621–638.
[10] MacKinnon, R. and Yellen, G. (1990) Science 250, 276–279.
[11] Hoshi, T., Zagotta, W.N. and Aldrich, R.W. (1991) Neuron 7, 547–556.
[12] Lopez, G.A., Jan, U.N. and Jan, L.Y. (1994) Nature 367, 179–182.